PREDICTING THE NO FORMATION IN NATURAL GAS COMBUSTION

André A. Isnard
Marcos S. P. Gomes
Pontifícia Universidade Católica do Rio de Janeiro, Departamento de Engenharia Mecânica, 22453-900, Rio de Janeiro, RJ, Brasil. E-mail: mspgomes@mec.puc-rio.br

Abstract

The work investigated a numerical procedure developed for simulating the combustion of natural gas in industrial furnaces, predicting thermal NO formation. It was based in the finite volume formulation and involved the k-e model of turbulence. The generalized finite rate model was used for simulating the combustion process, including limiting rate of reactions calculated by the Arrhenius or the Magnussen models. The discrete transfer radiation model was also employed. A simple one step reaction mechanism was used for representing the combustion of the fuel. The oxidation of nitrogen was simulated by considering the Zeldovich mechanism and by coupling NO formation and combustion. The fundamental goals of this research were (i) to evaluate the model efficiency by comparing its quantitative predictions with available experimental data and (ii) to relate the influence of the temperature field with the NO formation rate. The model results indicated a high dependence of the NO concentration on the temperature and the [O] radical fields. Further refinements will be necessary in future model developments for correctly predicting NO.

Key-words: Combustion Modeling, NO_x, Natural Gas

1. INTRODUCTION

In this work, it was investigated the performance of a model based in the finite volume formulation, including the k-ε model of turbulence, the generalized finite rate models of Arrhenius and Magnussen for chemical reactions calculations, and the discrete transfer radiation model, for simulating the combustion process in industrial furnaces.

In a natural gas combustion equipment, nitrogen oxide is formed mainly by oxidation of molecular nitrogen from the combustion air (thermal NO). The Zeldovich mechanism has been extensively tested and investigated in predicting thermal NO in such conditions. In these investigations, the assumption of equilibrium values for species and radicals concentrations is a simplification generally adopted, failing in estimating the NO formation rates near the combustion zone. The present work investigated the implication of implementing the Zeldovich mechanism by coupling the NO formation with the combustion process in a simplified reaction mechanism.

The purpose of this study was to investigate the performance of such a modeling approach in predicting NO formation in industrial natural gas flames. In this manner, the model may be used in evaluating the environmental impact of practical combustion units.

1.1 Zeldovich Mechanism of NO Formation

Zeldovich (1946) proposed a two reactions mechanism represented by reactions (1) and

(2). This mechanism is initiated by reaction (3), which represents the dissociation of molecular oxygen, in which M denotes a third body. M may be regarded as any species such as N_2, N, NO, O_2 or O, with the function of stabilizing the reaction. In our case, M was substituted by N_2, once this species was the most abundant in the interior of the furnace.

$$N_2 + O \underset{k_{1b}}{\overset{k_{1f}}{=}} NO + N \tag{1}$$

$$N + O_2 \underset{k_{2b}}{\overset{k_{2f}}{=}} NO + O \tag{2}$$

$$O_2 + M \underset{k_{3b}}{\overset{k_{3f}}{=}} O + O + M \tag{3}$$

In this mechanism proposed by Zeldovich, the combustion reaction is considered only as a source of energy for the reactants, as the reactions (1) and (2) occur independently of the combustion reaction. In this situation, NO formation rates are calculated assuming equilibrium values of temperature and concentration of O, N_2 and O_2. This process has been named by Zeldovich as a thermal mechanism.

Errors may be introduced by this approximation, mainly predicting NO formation rates near the combustion zone. In the present work it was investigated a simplified reaction mechanism implementing the Zeldovich one, coupling the NO formation process with the combustion process. This direct approach consists on the simultaneous calculations of the rate equations for reactions (1)-(3) and the rate equation describing the combustion process.

2. MODEL DESCRIPTION

We have used the commercial code Fluent to simulate the industrial furnace and the combustion process. A description of the models employed are presented in the next sections.

2.1 Turbulent Flow Field

The model implemented for simulating the turbulent flow was composed by the equation (4) for the conservation of total mass and the equation (5) for the conservation of momentum in the time averaged form. The Boussinesq's hypothesis was taken into account leading to an effective viscosity given by equation (6). Equation (7) represents the modified total pressure P, considering the contributions due to the turbulent fluctuations.

$$div(\rho \mathrm{v}) = 0 \tag{4}$$

$$div(\rho \mathrm{v}\,\mathrm{v}) = -grad\,P + div(\mu_{ef}\,grad\,\mathrm{v}) + div(\mu_{ef}\,grad\,\mathrm{v})^T \tag{5}$$

$$\mu_{ef} = \mu + \mu_t \tag{6}$$

$$P = p - \frac{2}{3}\left[\mu_{ef}\,div\,\mathrm{v} + \rho k\right] \tag{7}$$

For calculating the turbulent viscosity it was used the k-ε model of turbulence. In this model, k corresponds to the turbulence kinetic energy and ε corresponds to the dissipation for the turbulence kinetic energy. Two more equations representing the conservation for k and ε were solved.

The above equations were solved simultaneously providing results for the turbulent flow field.

2.2 Temperature Field

For simulating the temperature field within the furnace it was solved the equation (8) for the conservation of energy, in which the total enthalpy h is defined as the sum of the enthalpies of each species h_i weighted by its mass fraction m_i , represented by equation (9).

$$div(\rho \mathrm{v} h) = div\left[\left(\frac{\mu}{\mathrm{Pr}} + \frac{\mu_t}{\mathrm{Pr}_t}\right) grad\, h\right] + \mathrm{v} \bullet grad\ p + S_h \tag{8}$$

$$h = \sum_i m_i h_i \tag{9}$$

Equation (10) represents the enthalpy source S_h due to the chemical reactions and the radiation heat transfer.

$$S_h = S_{reac} + S_{rad} \tag{10}$$

2.3 Chemical Species and Combustion Modeling

For simulating the transport in the gas phase, the mixture was considered as an ideal gas, and a set of conservation equations for the chemical species was solved. Equation (11) represents the conservation for each chemical species.

$$div(\rho \mathrm{v} m_i) = div\left[\left(\frac{\mu}{Sc} + \frac{\mu_t}{Sc_t}\right) grad\, m_i\right] + R_i \tag{11}$$

In the above equation, the term R_i represents the source for each species. It may be expressed by the sum of the reaction rates (generation or consumption) for species i in every reaction k, as denoted by $R_{i,k}$ corresponding to equation (12).

$$R_i = \sum_k R_{i,k} \tag{12}$$

The rates in the combustion reactions were calculated by using both the Arrhenius and the Magnussen models (Fluent User's Guide, 1996). In the Arrhenius model, the reaction rate may be computed according to equation (13).

$$R_{i,k} = \eta_{i,k}\, M_i\, T^{\beta_k}\, A_k \exp\left(-E_k / RT\right) \prod_j C_j^{\gamma_{j,k}} \tag{13}$$

In the Magnussen model, the rate of reaction is calculated both by equations (14) and (15) and the smallest value is taken (limiting rate). In these expressions, j* represents the reactant which gives the smallest value for $R_{i,k}$, and K_1 and K_2 are empirical constants.

$$R_{i,k} = \eta_{i,k} M_i K_1 \rho \frac{\varepsilon}{k} \frac{m_{j^*}}{\eta_{j^*,k} M_{j^*}} \tag{14}$$

$$R_{i,k} = \eta_{i,k} M_i K_1 K_2 \rho \frac{\varepsilon}{k} \frac{\sum_p m_p}{\sum_p \eta_{p,k} M_p} \tag{15}$$

The smallest value obtained in the two models, Arrhenius and Magnussen, was employed as the final value for the reaction rate in the calculation of the source term due to chemical reactions involving species i, R_i.

2.4 Radiation Model

The Discrete Transfer Radiation Model (DTRM) was employed in the computation of the heat fluxes due to radiation. In this model, the change in the radiant intensity I, integrated over all wavelengths, along a path S, is calculated according to equation (16) when scattering is neglected.

$$\frac{dI}{dS} = -\alpha I + \frac{\alpha \sigma T^4}{\pi} \tag{16}$$

The terms on the right side of equation (16) represent the loss by absorption and the gain by emission due to the participating medium, respectively .

3. PROBLEM SET-UP

3.1 Geometry

The geometry which was simulated, corresponding to a cylindrical combustor, is shown in Figure 1. It was the same geometry used by Garreton (1994) in its experiments. The computational domain was divided into 60 control volumes in the axial direction and 30 control volumes in the radial direction. A non-uniform grid was employed so that high resolution was obtained around the jets and next to the walls.

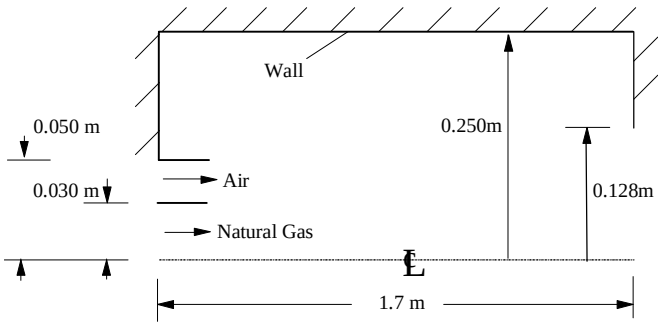

Figure 1. Schematic of the cylindrical furnace.

3.2 Inputs to the Model

The cylindrical combustor, illustrated in Figure 1, may be modeled as axisymmetric, a simplification which was implemented in the burner geometry so that the problem could be treated as two-dimensional.

Natural gas was used as the fuel. Taking into consideration that the major component of the natural gas is methane, it was assumed that the combustion reaction taking place inside the furnace could be represented by the equation for the oxidation of methane. The finite rate combustion was modeled using a global one-step reaction mechanism (reaction (17)), assuming complete conversion of the fuel to CO_2 and H_2O. The chemical reactions model was represented by reaction (17) plus reactions (1), (2) and (3) for the NO formation corresponding to the Zeldovich mechanism.

$$CH_4 + 2O_2 \xrightarrow{k_{17}} CO_2 + 2H_2O \qquad (17)$$

The parameters used in the reactions calculations are presented in Table 1.

Table 1. Parameters used in the reactions calculations

Const. Rate	Forward Reaction $cm^3\ molecule^{-1}\ sec^{-1}$	Reverse Reaction $cm^3\ molec^{-1}\ sec^{-1}$
k_1	$1.16 \times 10^{-10}\ \exp(-75500/RT)$	2.57×10^{-11}
k_2	$2.21 \times 10^{-14}\ T \times \exp(-7080/RT)$	$5.3 \times 10^{-15}\ T \times \exp(-39100/RT)$
k_3	$1.876 \times 10^{-6}\ T^{-1/2} \times \exp(-118000/RT)$	2.6×10^{-33a}
k_{17}	$1.667 \times 10^{-9}\ \exp(23900/RT)$	---------

[a]Third-order reaction, $cm^6\ molecule^{-2}\ sec^{-1}$

The considered flame was a turbulent diffusion flame. A nozzle in the center of the combustor introduced natural gas at 0.0125 kg/s. Ambient air entered the combustor coaxially at 0.186 kg/s. The AF ratio is near stoichiometric (about 5% excess fuel). The Reynolds number based on the natural gas jet diameter was approximately 29000.

The natural gas jet was given an inlet temperature of 313K, a methane mass fraction of 0.9, a nitrogen mass fraction of 0.1, a turbulence intensity and length scale of 10% and 0.03m. The air inlet was given a temperature of 323K, oxygen, nitrogen and vapor mass fractions of 0.23, 0.76 and 0.01 respectively, a turbulence intensity and length scale of 6% and 0.04 m.

The constants used in k-ε model were c_1 =1.4, c_2 = 1.9 and c_μ = 0.09. The turbulent Prandtl and Schmidt numbers were set at 0.5. In the Magnussen model the constants K_1 was equal to 4.0 and K_2 was equal to 0.5. The density of the gaseous mixture was calculated by using the ideal gas law, according to equation (18) below, where p_{op} is the average operation pressure inside the furnace. It was assumed that p_{op} was equal to one atmosphere.

$$\rho = \frac{p_{op}}{RT\sum_i m_i / M_i} \qquad (18)$$

Two cases were simulated for comparison, the only difference between them was in the thermal flux boundary condition.

In Case 1 the thermal flux cross the furnace wall was prescribed according to values determined through measurements of the heat removed by cooling jackets. Table 2 presents the heat flux values on the side walls determined along the combustor for Case 1. On the frontal walls, heat flux values were estimated as 26.1 kW/m^2 to the wall close to the jets inlets and 78.9 kW/m^2 to the wall close to the gases exit.

Table 2. Thermal flux prescribed on the furnace wall for Case 1

Section (mm)	Heat Flux (kW/m^2)
0 < x < 380	26.1
380 < x < 680	39.7
680 < x < 980	59.6
980 < x < 1280	88.3
1280 < x < 1400	95.3
1400 < x < 1700	102.2

For Case 2 the furnace outer walls were treated as adiabatic surfaces by imposing a zero heat flux in the setting-up of the boundary conditions for the thermal problem.

The purpose of comparing the results for Cases 1 and 2 was uniquely to identify the influence of the temperature field on the thermal-NO formation model that was being investigated.

4. RESULTS

Case 1:

Figure 2 shows that the peak of the predicted temperature in the flame reaches approximately 1900 K. Comparing these results with the experimental data it is clear that such high temperatures are overestimated. One of the possible reasons for explaining this difference is the fact that the one-step combustion reaction (17) which was employed in the simulation is a very simplified approach for solving the problem. Detailed reaction mechanisms, which include dissociation reactions, are important for more accurate temperature predictions. In a more recent work, it was found that the inclusion of a two-step model for combustion highly improves the quality of the predictions.

.

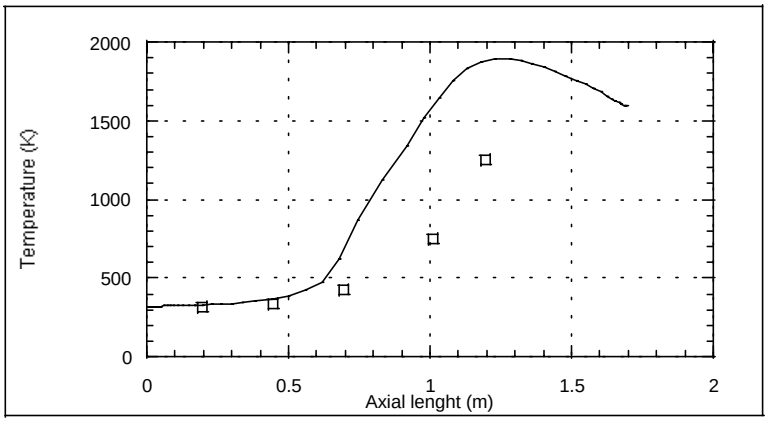

Figure 2. Comparison between predicted (line) and experimental (squares) temperature along the symmetry axis of the furnace.

Figures 3 and 4 show, respectively, the O_2, and CO_2 mole fraction fields in the combustor. It can be seen that the trends for the O_2 mole fraction predictions and the CO_2 formation from the combustion reaction are in reasonable agreement with the experimental trends.

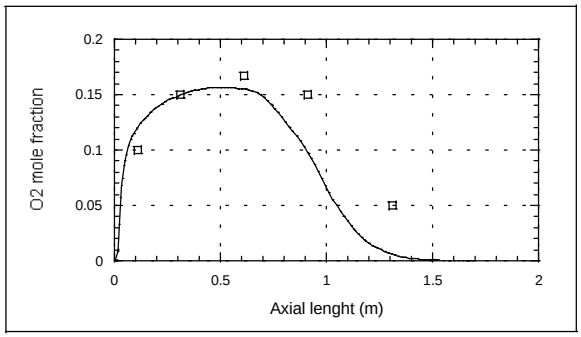

Figure 3. Comparison between predicted (line) and experimental (squares) Oxygen mole fraction along the symmetry axis of the furnace.

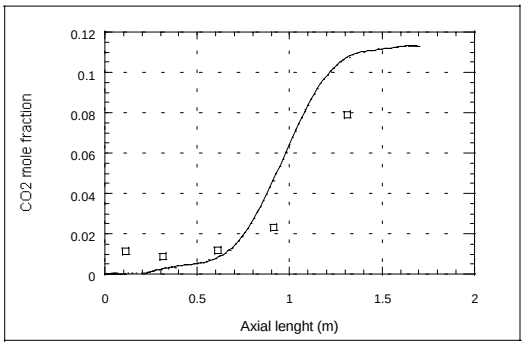

Figure 4. Comparison between predicted (line) and experimental (squares) Carbon Dioxide mole fraction along the symmetry axis of the furnace.

Figure 5 presents the temperature, [O] mole fraction and NO mole fraction fields for Case 1. The peak of [O] mole fraction reaches 63.5 ppb and occurs at the front flame region while the peak of NO mole fraction occurs at exit of the combustor. The maximum value for the predicted NO concentration reaches 0.3 ppb. In Garreton (1994), the maximum experimental value for the measured NO concentration reaches 18 ppm, for the same geometry and conditions simulated in Case 1. Therefore, the concentration levels for the predicted NO were unrealistically small comparing with the experimental data. However, the results are in qualitative accordance with the literature. Seinfeld (1986) indicates that the maximum NO concentration levels occur after the flame region, where the combustion reaction has already reached chemical equilibrium.

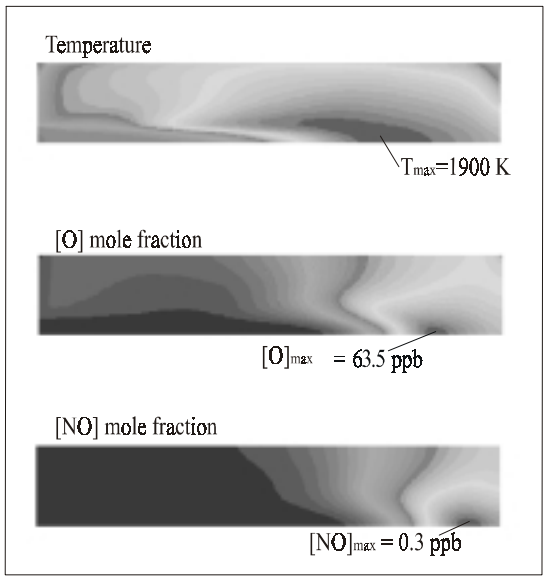

Figure 5. Temperature, [O] mole fraction and [NO] mole fraction fields to Case 1.

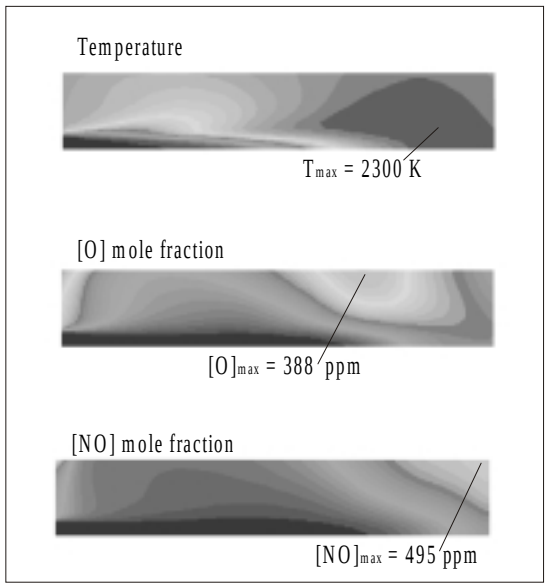

Figure 6. Temperature, [O] mole fraction and [NO] mole fraction fields to Case 2.

Case 2:

Figure 6 above shows the temperature, [O] mole fraction and NO mole fraction fields within the furnace for the adiabatic situation. The peak temperature in the flame reaches approximately 2300 K in the flame front region, a value 400 K above that for Case 1. The [O] mole fraction peak reaches 388 ppm, a number approximately 10^4 times greater than that one found in Case 1. The maximum NO concentration reaches 495 ppm, a value 10^6 times greater than that observed in Case 1. As it was expected, the thermal-NO is extremely dependent on the temperature. For a 400 K variation in the maximum temperature value, it was observed a gain of 10^6 times in the concentrations levels predicted for NO, comparing Case 1 and Case 2.

It was not presented comparison between Case 2 results and experimental data because the purpose of simulating Case 2 was uniquely to verify the influence of the temperature field on the NO formation, by comparisons between Cases 1 and 2.

Another important point is the great variation of the [O] radical concentration predicted in Cases 1 and 2, indicating that the [O] radical formation is also very influenced by temperature. This fact is understood as reaction (4), the oxygen dissociation reaction, presents high activation energy and is strongly dependent of temperature.

5. CONCLUSION

The introduction of a model which prescribes the heat fluxes at the furnace walls impacts significantly in the prediction of the temperature field, when compared with the adiabatic situation.

Comparing Case 1 and Case 2 results, for a 400 K variation in the maximum temperature value, it was observed a gain of 10^4 times for the [O] concentrations levels and a gain of 10^6 times for the concentrations levels predicted for NO. These results indicate a strong influence of the temperature in the concentrations of [O] and NO within the furnace.

Bilger et al. suggest that in turbulent diffusive flames, the impact of the [O] (monatomic oxygen) radical in NO formation rate is very important. Therefore, to the temperatures levels observed in Case 1, the formation of radical [O] exclusively by reaction (4), the oxygen dissociation reaction, seems to be insufficient for representing reality reasonably and a different approach will be necessary. Possible alternatives are: (i) the use of a detailed chemical mechanism, in which a larger number of chemical kinetic equations involving other intermediate species will be considered, and (ii) a simplification in the real kinetic process by adopting equilibrium values for the [O] radical concentration.

As a consequence of the implementations in the present model, the NO formation is underestimated and the thermal-NO mechanism, as adopted, has a poor performance. Another possibility for improvement relies in the fact that the mixture has excess fuel, near to stoichiometric, and the temperatures are low (< 1500 K). Therefore, it would be recommended the implementation of both the extended Zeldovich mechanism and the Prompt-NO mechanism.

Carrying on with this study, other approaches to the prediction of [O] concentration, as well as more sophisticated models for NO formation, are being implemented for further comparisons with the experimental data. In an attempt to improve the temperature field predictions, a combustion mechanism in two steps is being tested with success, allowing for the evaluation of [CO] formation.

6. NOMENCLATURE

A	Pre-exponential Factor	E	Activation Energy
C	Molar Concentration	I	Radiation Intensity

M Molecular Weight
P Modified Total Pressure
Pr Prandtl Number
R Reaction Rate or Universal Gas Constant
Sc Schimidt Number
T Temperature
c_μ Turbulent Viscosity Coefficient
g Gravity Acceleration
h Enthalpy
k Turbulent Kinetic Energy
m Mass Fraction
p Pressure
v Velocity Vector

Greek Symbols

α Absorption Coefficient
β Temperature Exponent
ε Rate of Dissipation of Turbulent Kinetic Energy or Total emissivity
γ Concentration Exponent
η Stoichiometric Coefficient
μ Absolute Viscosity
ρ Specific Mass
σ Stefan Boltzmann Constant

Subscripts

ef Effective Viscosity
i Species
j Reactant Species
k Reaction
p Product Species
t Turbulent Viscosity, Prandlt and Schmidt Numbers

7. REFERENCES

- Bilger, R.W., and Beck, R.E., Fifteenth Symposium (Int) on Combustion, The Combustion Institute, Pittsburgh, p 541, 1975.
- Bowman, Craig T. and Miller, James A., 1989, "Mechanism and Modeling of Nitrogen Chemistry in Combustion", Progress in Energy Combustion Science.
- Fluent User's Guide, version 4.3, Fluent Incorporated, New Hampshire, March 1995.
- Garreton, D., Simonin, º, First Workshop on Aerodynamics of Steady State Combustion Chambers and Furnaces: Final Results, October 17-18, 1994, Chatou, France.
- Gomes, Marcos S. P., Nieckele, Angela O., Naccache, Monica F. and Kobayashi, William T., "Numerical Investigation of the Oxygen Enriched Combustion Process in a Cylindrical Furnace", Fourth International Conference on Technologies and Combustion for a Clean Environment, July -1997, Lisboa , Portugal.
- Isnard, A, Gomes, M.S.P., Numerical Investigations on the NOx Formation in Natural Gas Combustion, 7th Brazillian Congress of Engineering and Thermal Sciences, November 3-6, 1998, Rio de Janeiro, Brasil.
- Konnov, A.A., "NO Formation Rates in Natural Gas Combustion", Fourth International Conference on Technologies and Combustion for a Clean Environment, July -1997, Lisboa , Portugal.
- Magel, H. C., Schnell,U. and Hein, K.R.G., "Modelling of Hydrocarbon and Nitrogen Chemistry in Turbulent Combustor Flows Using Detailed Reactions Mechanisms", 3rd Workshop on Modelling of Chemical Reaction Systems, Heidelberg, 1996.
- Patankar, S.V., 1980, Numerical Heat Transfer and Fluid Flow. Hemisphere Publishing Corporation, New York.
- Seinfeld's, John H., 1986, Atmospheric Chemistry and Physics of Air Pollution, John Wiley & Sons, New York.
- Tomeczek, J. and Gradón,B, "The Rate of Nitric Oxide Formation in Hydrocarbon Flames", Fourth International Conference on Technologies and Combustion for a Clean Environment, July -1997, Lisboa , Portugal.